Assessing tumour extent and heterogeneity on T1-weighted 3D DCE-MRI of the Breast: Comparative study of the Computational Fat Suppression Algorithm, and Quantitative Pharmacokinetic (PK) modelling

M. Khazen[1], J. D'Arcy[1], D. J. Collins[1], A. R. Padhani[2], P. Kessar[1], M. O. Leach[1]

[1]Cancer Research UK Clinical Magnetic Resonance Research Group, Institute of Cancer Research and The Royal Marsden NHS Trust, Sutton, Surrey, United Kingdom, [2]Paul Strickland Scanner Centre, Mount Vernon Hospital, Northwood, United Kingdom

Introduction. Effective assessment of tumour shape and structure is of significant importance for the diagnosis of breast cancer on dynamic contrast enhanced (DCE) MRI. Using the whole range of the consecutively acquired volumes in 3D DCE-MRI measurement, the Computational Fat Suppression (CFS) algorithm [1] automatically segments breast tissues into three groups: fat, tissues of persistent enhancement, and remaining enhancing tissues producing washout phase (or beginning of the washout phase – the plateau) during the measurement time. In this study we compare the results of the CFS algorithm with the results of quantitative pharmacokinetic (PK) modelling, for the purpose of assessing how well the CFS algorithm discriminates persistent and non-persistent uptake in tissues, and its potential applicability for identification of tumour extent and structure.

Materials and Methods. Ten DCE-MRI measurements of different patients of the symptomatic cohort of women participating in the UK multicentre trial of MRI in women at high risk of breast cancer (MARIBS, [2]) all performed at the same medical centre were selected. Four studies were later excluded on the basis of poor quality (n=2), and poor contrast enhancement or motion at the site of the lesion (n=2). The CFS algorithm and the PK analysis were applied to 6 cases; 2 with benign lesions and 4 with malignant (all diagnoses were confirmed pathologically). The measurements were performed using a Siemens 1.5T Vision scanner with 3D T1-weighted fast spoiled gradient echo sequence with a temporal resolution 90 sec and a spatial resolution 1.33 x 1.33 x 2.5 mm (matrix size 256 x 128 X 64). Each study acquired two pre-contrast and five post-contrast datasets after bolus injection of Gd-DTPA at 0.2 mmol/kg of body weight. Proton density measurements were obtained for each patient to enable calculation of T1, which is necessary for PK modelling. A calibration was performed using phantoms to produce a curve of true T1 values versus the ratio of T1-weighted to proton density signal intensity, converting signal-intensity uptake into a Gd-DTPA concentration. For each patient the tumour extent was outlined by a radiologist on subtracted post-contrast images. Independently, the CFS algorithm was applied to the whole imaged volume. The segmentation at the site of the lesion was compared with the outline defined by the radiologist to assess the accuracy of the algorithm. A rectangular ROI encompassing the lesion on one of the slices was then selected. The original uptake curves of the voxels within the ROI that are not classified as fat by the CFS algorithm were used for PK modelling based on the Tofts and Kermode model [3]. For each ROI maps of transfer constant (K^{trans}, [4]) were produced and correlated with the results of the CFS. (For the PK modelling, the decay of Gd-DTPA concentration in the blood plasma compartment was assumed as defined by Winemann [5].)

Results. In all the cases, the results of the CFS algorithm were anatomically consistent with the outlines of radiologist. In addition, the heterogeneity of lesions was reflected in the values of the CFS map (Fig. 1). The detected heterogeneous structure of lesions was significantly correlated with computed maps of transfer constant (Fig. 2.).

Conclusions. Existing approaches to detection of abnormal tissues on DCE-MRI of the breast typically include the use of dimension reduction techniques often utilising a subset of three time-points (i.e. three volumes) from the range of consecutively acquired volumes (e.g. [6]). The CFS algorithm uses the whole range of available time-points. This improves the robustness of the algorithm, as shown by the good agreement with pharmacokinetic modelling. Further work will involve comparison of the methods applied to clinically validated datasets, in particular to 3D data with better temporal resolution. In this study, we use values of K^{trans} only to deploy the relative function of tissues segmented by the CFS. It should be noted, that in general using the data of 90 sec. temporal resolution would underestimate the value of K^{trans} typically found in breast Ca by approximately 20%. (That has been confirmed by both simulation and measurement comparing with fast 2D data from the same subject.)

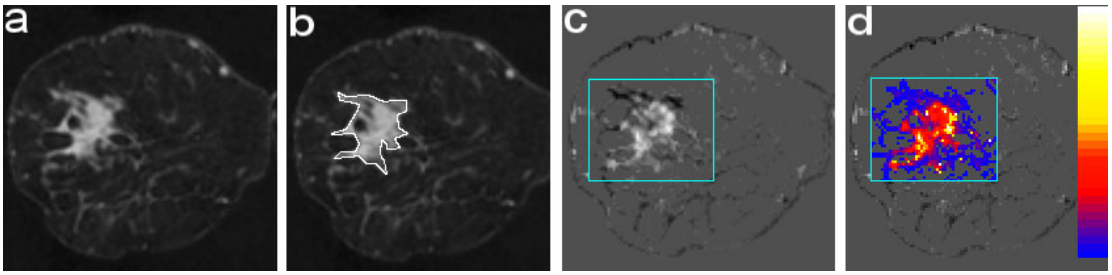

Fig. 1. Coronal T1-weighted image at the site of the lesion (mixed carcinoma, grade II)
- (a) Subtracted image acquired at 4.5 min post administration of Gd-DTPA
- (b) Extent of the lesion, as outlined by a radiologist
- (c) Result of the Computational Fat Suppression algorithm – the CFS map. Three groups of tissue are present: fat (outlined by background mid-grey colour, corresponding to the value of zero on the CFS map), persistent enhancement (dark grey, corresponding to negative values of the CFS map), and wash-out (bright grey – positive values of the CFS map)
- (d) Map of transfer constant at the selected ROI (boxed on (c) and (d) images)

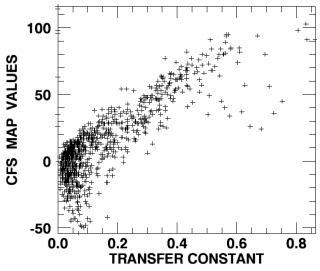

Fig. 2. Association plot of the values of K^{trans} and the corresponded values of computational fat suppression image for the ROI in Fig. 1. P-value: $p < 0.000001$ (based on rank correlation)

Acknowledgements The support of Medical Research Council (MRC) UK, and Cancer Research UK is gratefully acknowledged.

References

1. Khazen M, Leach MO. Excitation independent far suppression for DCE-MRI of Breast Cancer, using a multivariate statistical approach. Proc. Intl. Soc. Mag. Reson. Med. 11 (2004) 830
2. The UK Breast Screening Study Advisory Group. Magnetic resonance imaging screening in women at genetic risk of breast cancer: imaging and analysis protocol for the UK multicentre study. Magnetic Resonance Imaging 18 (2000), 765-776
3. Tofts P, Kermode AG. Measurement of the Blood-Brain Barrier Permeability and Leakage Space using Dynamic MR Imaging. 1. Fundamental Concepts. Magn. Reson. Med. 1991(17):357-367
4. Tofts PS, Brix G, Buckley DL, et. al. Estimating Kinetic Parameters From Dynamic Contrast-Enhanced T1-Weighted MRI of a Diffusable Tracer: Standardized Quantities and Symbols. J. Magn. Reson. Imaging 1999; 10:223-232
5. Weinmann HJ, Laniado M, Muetzel W. Pharmacokinetics of Gd-DTPA/dimeglumine After Intravenous Injection Into Healthy Volunteers. Phys. Chem. Phys. Med. NMR 1984,16:167
6. Degani H, Gusis V, et. al. Mapping pathophysiological features of breast tumors by MRI at high spatial resolution. Nat Med 1994; 3:780-782